

THE PENNSYLVANIA STATE UNIVERSITY
SCHREYER HONORS COLLEGE

DEPARTMENT OF CHEMICAL ENGINEERING

Analysis of Operating Conditions for Commercially Available Depth Filters

KEVIN DYKE
FALL 2023

A thesis
submitted in partial fulfillment
of the requirements
for a baccalaureate degree
in Chemical Engineering
with honors in Chemical Engineering

Reviewed and approved* by the following:

Andrew Zydney
Professor of Chemical Engineering
Thesis Supervisor

Ali Borhan
Professor of Chemical Engineering
Honors Adviser

* Electronic approvals are on file.

ABSTRACT

Depth filtration is used extensively for the purification of biological products. There are many commercially available depth filters that exploit differences in size and intermolecular interactions to achieve important separations. However, there is currently a lack of understanding of how these depth filters perform under a wide range of operating conditions. The objective of this thesis is to evaluate the performance of several commercial depth filters with the goal of understanding how these depth filters might be used more effectively to purify biological products made using Chinese hamster ovary (CHO) cells.

Experiments were performed using a series of model proteins with the A1HC, D0SP, and X0SP depth filters manufactured by Millipore Sigma. Protein concentrations were evaluated using a spectrophotometer based on UV absorbance measurements or the Bradford assay. These studies showed that the solution pH and protein isoelectric point (pI) have little effect on the binding capacity of the A1HC filter, suggesting that this filter binds protein primarily through hydrophobic interactions, while increasing protein pI at acidic conditions significantly increases the binding capacity of the X0SP and D0SP filters, both of which appear to bind proteins primarily through electrostatic interactions. It was also found that flow rate does not impact the binding capacity of the A1HC, and that actual host cell proteins (HCP) from CHO cells can be effectively removed by these depth filters. These results provide important insights into the performance characteristics of these depth filters and how they can be used more effectively for depth filtration processes.

TABLE OF CONTENTS

LIST OF FIGURES	iii
LIST OF TABLES	iv
ACKNOWLEDGEMENTS	v
Chapter 1 Introduction	1
Principles of Depth Filtration	1
Industry Applications	3
Objectives	5
Chapter 2 Materials and Methods	6
Buffer Preparation	6
Protein Solution Preparation	7
Depth Filtration Setup	8
Protein Concentration Measurements	10
Bradford Assay	11
Chapter 3 Results and Discussion	13
Effect of pH	13
Effect of Flow Rate	21
HCP Binding	22
Chapter 4 Conclusions	24
Chapter 5 References	26
ACADEMIC VITA	28

LIST OF FIGURES

Figure 1. Depth filter diagram. Taken from [7].	1
Figure 2. Depth filtration purification phenomena: (a) sieving, (b) interception, (c) adsorption. Taken from [6].	2
Figure 3. Schematic of initial clarification steps in downstream bioprocessing. Taken from [8]......	4
Figure 4. Depth filtration setup.	10
Figure 5. Bradford assay standard curve. Taken from [1].	12
Figure 6. Absorbance profiles for albumin processed at various pH conditions using the (a) A1HC, (b) D0SP, and (c) X0SP filter.	15
Figure 7. Absorbance profiles for myoglobin processed at various pH conditions using the (a) A1HC, (b) D0SP, and (c) X0SP filter.	17
Figure 8. Absorbance profiles for alpha-chymotrypsin processed at pH 4.5 and 6 using the A1HC filter.	18
Figure 9. Binding capacities as a function of pH for the different depth filters for (a) albumin, (b) myoglobin, and (c) alpha-chymotrypsin.	20
Figure 10. A1HC breakthrough profiles for ovalbumin at 50, 150, and 300 LMH.	22
Figure 11. Breakthrough curve for HCP during filtration through the A1HC depth filter.	23

LIST OF TABLES

Table 1. Model protein information.....	8
Table 2. Depth filter summary.....	10

ACKNOWLEDGEMENTS

Completing this thesis was a very rewarding, yet challenging process that required significant amounts of effort and perseverance and I could not have done it without the tremendous support I received throughout its entirety. First, I would like to thank Dr. Andrew Zydney for accepting me into his lab in September 2022 and allowing me to conduct research for him. He is one of the great science minds in the field of bioprocessing and has been a great mentor. I would not have accomplished this without his invaluable guidance along each step of the way.

The next person I would like to thank is Liang-Kai Chu, a PhD candidate under Dr. Zydney. Over the past year I had the opportunity to work with Liang-Kai extensively, and he played a crucial role in my development as a researcher and chemical engineer. I learned a lot about designing effective experiments, accurately conducting them, and then analyzing their results from him. I am very thankful for the significant amount of time and effort he invested in me; I would never have been able to complete this thesis without him.

Dr. Stephanie Velegol was the first professor to take a chance on me early in my academic career and invited me to join her research lab when I had little to no professional experience. This was extremely beneficial, and I am beyond grateful for everything she has done for me. Although I no longer work directly under Dr. Velegol, she has continued to aid in my development and has been there whenever I needed something from her. She is a great professor and an even better person.

Finally, I would like to thank my family and friends for their constant support through the highs and lows of my undergraduate career. It has not been an easy process, but it has been

extremely rewarding and I want to thank Penn State's department of chemical engineering and the Schreyer Honors College for giving me this opportunity.

Chapter 1

Introduction

Principles of Depth Filtration

Depth filtration is a method of filtration that removes particles and impurities throughout the entire depth of a porous medium. It is a powerful and widely used separation technique that has a long history, with texts describing the use of depth filtration in the production of potable drinking water from as far back as 1500 BCE.¹¹ Depth filters also have applications in many current industries, with their use in downstream bioprocessing for the production of high value biopharmaceuticals being one of the largest. Most membranes are designed to retain impurities at the surface of the porous medium, which can limit their capacity as surface pores become blocked. Depth filters can have much higher binding capacities and can remove more impurities based on electrostatic and hydrophobic interactions within the depth of their porous medium. The feed travels through the depth filter medium, passing through tangled pores of differing sizes and interactions.

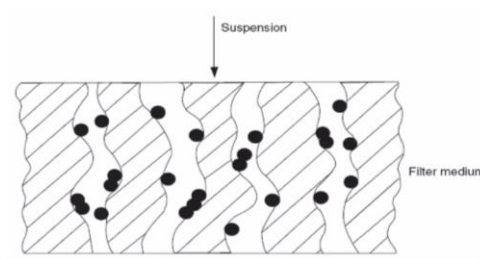


Figure 1. Depth filter diagram. Taken from [7].

Depth filters purify the feed by retaining impurities in their medium either through size and/or intermolecular interactions. Particle sieving occurs when the impurities/particles are larger than the pore spaces in the medium so that they cannot pass through into the permeate.⁶

Interception can also occur due to the layout and shape of the depth filter's pores as the particle gets stuck in the medium due to its highly tortuous flow path. Separations based on intermolecular interactions occur when the impurities adhere to, or bind to, the solid surfaces within the depth filter. This is achieved in most depth filters through electrostatic or hydrophobic interactions. Electrostatic interactions take advantage of surfaces that are of opposite charge to the impurities. Hydrophobic interactions occur between regions of the depth filter medium and impurities with nonpolar groups.

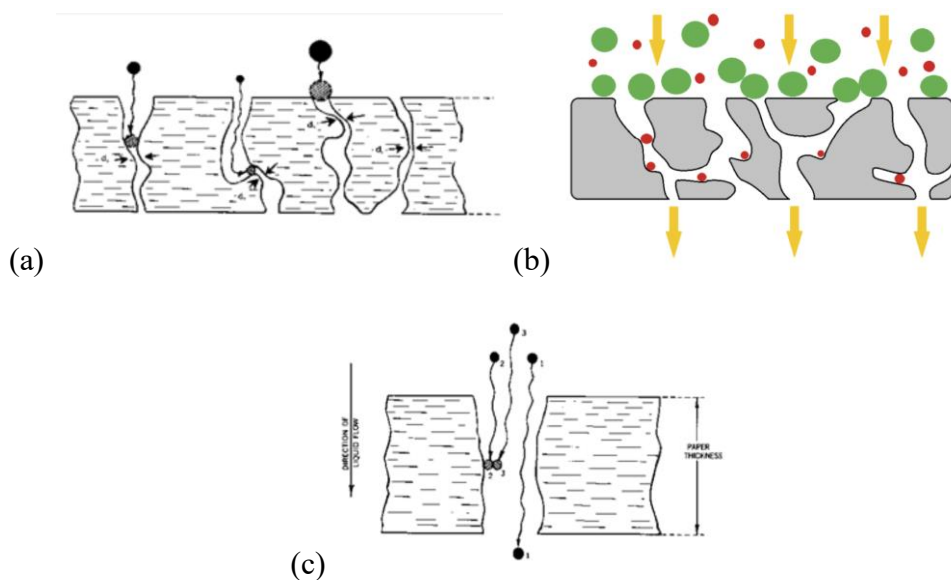


Figure 2. Depth filtration purification phenomena: (a) sieving, (b) interception, (c) adsorption. Taken from [6].

The composition and design of the depth filter medium determines its purification capabilities. Each depth filter is designed with a specific purpose and to remove a specific type

of impurity. For instance, in bioprocessing, most depth filter media contain cellulose or polypropylene fibers in combination with a filter aid, such as diatomaceous earth, activated carbon, or perlite.² These media are used in bioprocessing because they can engage in multiple types of intermolecular interactions and provide a high surface area for enhanced impurity removal.

The performance of these depth filters is a function of how effectively they remove specific impurities and the overall capacity they can provide in a given process. This performance is heavily influenced by the depth filter's operating conditions, including the pH and conductivity of the feed solution. These conditions can influence the binding capacity of the depth filter and whether an impurity travels through the depth filter and into the permeate without being retained. The effect of these operating conditions on the performance of a depth filter is difficult to predict since it depends on the details of the feed material and depth filter media, meaning that experimental process optimization is typically needed to develop effective depth filtration processes. Operating a depth filter at improper pH conditions can diminish the efficiency and shorten the lifespan of the filter. Lower conductivities typically result in a higher level of impurity removal due to electrostatic interactions, however the product can also be bound by the depth filter decreasing the overall yield of the process.

Industry Applications

As previously stated, depth filtration is widely used in bioprocessing for the manufacturing of different medicines, specifically in downstream purification of products made using fermentation or mammalian cell culture. When used in this setting, depth filters are

typically designed to provide initial clarification of the cell culture fluid by removing cells and cell debris.⁵ These depth filters can effectively protect subsequent chromatography steps in the downstream purification process from rapid fouling/clogging.

Several studies have also shown that depth filters can remove significant amounts of DNA, HCP, and viruses depending on depth filter medium and the pH and conductivity conditions.⁹ The goal of the depth filter in this type of process is purification of the product without compromising its yield or potency. Depth filters are available in a wide range of sizes so that they can be employed from bench-top experiments to large-scale commercial manufacturing, with external surface areas ranging from 10 cm² to more than 10-15 m². Another advantage of depth filters in industry is that they are single-use devices. This provides a lot of flexibility and ease of operation, particularly when used at large scales.

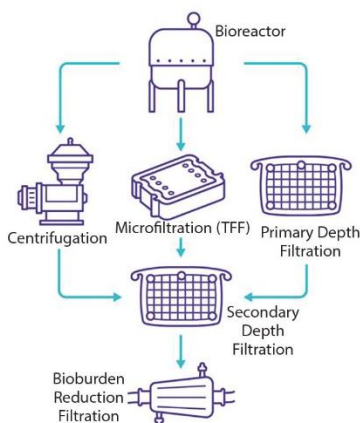


Figure 3. Schematic of initial clarification steps in downstream bioprocessing. Taken from [8].

Objectives

This thesis aims to further evaluate several commercially available depth filters under a range of conditions to understand how they can be used more effectively. Specifically, data were obtained at different pH and flow rate using model proteins of differing isoelectric points (pIs). These results were then compared with data for the removal of CHP cell HCP to get a better idea of how these depth filters would perform in the purification of CHO-derived biological products.

Chapter 2

Materials and Methods

Buffer Preparation

For all experiments described in this thesis, the necessary buffers were prepared in the laboratory from stock solutions or from the individual buffer components. When prepared from stock solutions, a highly concentrated solution of the desired buffer was diluted with deionized (DI) water to achieve the target concentration. For instance, all 0.3x and 1x phosphate-buffered saline (PBS) buffers were prepared by the appropriate dilution of a 10x PBS stock solution. To determine the dilution volume, the following equation was used:

$$M_1V_1 = M_2V_2 \quad (1)$$

where M is the buffer concentration, V is the buffer volume, and 1 and 2 designate the initial and final conditions, respectively. When prepared from the buffer components, a specific mass of each salt and its corresponding acid/base, determined from the target concentration and the molecular weight, was measured using a digital scale and then dissolved into DI water using a stir plate and stir bar.

To achieve the desired pH, an acid or base was slowly added to the buffer solution using a pipet. After each addition of acid or base, the solution was stirred, and its pH was measured using a pH meter. This was repeated until the target pH was achieved. Acids were used to lower the pH, most frequently 5M hydrochloric acid. Bases were used to raise the pH, most frequently 5M sodium hydroxide. These highly concentrated acids and bases were used to reduce the volume that needed to be added and thus minimize the dilution of the other buffer components.

The conductivity was adjusted by adding aqueous sodium chloride (NaCl) or DI water to the buffer solution and then evaluating its conductivity using a conductivity meter. NaCl was added to raise the buffer's conductivity and DI water was added to reduce the buffer's conductivity.

Protein Solution Preparation

Depth filtration experiments were performed with a series of model proteins. The model proteins were purchased as powders and either stored between 2-8°C or below 0°C. To prepare the protein solution, a measured mass of the model protein was mixed with a buffer (typically 0.3x PBS) using a stir bar, similar to the procedure used to prepare buffers. The volume of buffer and mass of protein used was dependent on the target concentration of the protein solution. After the model protein was completely dissolved, the solution was vacuum filtered through a 0.2-micron pore size filter. This is to ensure the absence of bacteria and particulate matter in the protein solution. The properties of the model proteins used in this thesis- albumin, myoglobin, alpha chymotrypsin, and ovalbumin- are summarized in Table 1.

Table 1. Model protein information.

Model Protein	Information	Supplier: Product #
Albumin	From bovine serum, pI ~4.8-4.9, stored at 2-8°C	Millipore Sigma: A2153-50G
Myoglobin	From equine skeletal muscle, pI 7, stored at 2-8°C	Millipore Sigma: M0630-5G
Alpha-Chymotrypsin	From bovine pancreas, pI 8.8, stored at <0°C	Millipore Sigma: C4129-1G
Ovalbumin	From chicken egg white, pI 5.2, stored at 2-8°C	Millipore Sigma: C7786-1G

Depth Filtration Setup

For all experiments, a 23 cm² depth filter purchased from Millipore Sigma was used. The depth filters were classified based on their pore size and underlying chemistry (A1HC, X0SP, and D0SP) as summarized in Table 2. The first two digits of the depth filter's name refers to its pore size and the last two digits of its name refers to its medium composition. The depth filters that end in "-SP" are composed of synthetic silica particles and polyacrylic fibers while the depth filters that end in "-HC" are composed of diatomaceous earth and cellulose fibers. To set up the depth filter for operation, tubing was attached to its inlet port and to its vent port, while the outlet port remained closed. The tubing attached to the vent port is only long enough to direct the retentate into a waste container and the tubing attached to the inlet has to be long enough to feed through a pressure gauge, peristaltic pump, and then into the feed container. The peristaltic pump is used to pump the feed into the depth filter so the inlet tube must be long enough to reach the

bottom of the feed container, ensuring all the feed solution is used and no air is pumped into the depth filter.

After the setup is complete, the depth filter was equilibrated by pumping equilibration buffer (the solvent used in the protein solution) through the depth filter, for at least twice the hold-up volume of the depth filter capsule. While the depth filter is equilibrating, it is tapped to remove any air bubbles, ensuring complete access to the surface area of the depth filter. Once equilibration buffer begins to elute from the vent tube, the pump was paused, and the tubing was removed from the vent port to be placed on the outlet port. The pump was restarted while continuing to tap the depth filter to remove any additional air bubbles. Once buffer begins to elute from the outlet port, there are no bubbles visible in the system, and the required volume of equilibration buffer has been processed, the depth filter is ready for use.

Place the inlet line into your feed material, disconnect the inlet tube from the depth filter, and start the pump so that the tubing is fully primed with the feed material. Reconnect the inlet tube to the depth filter and begin the pump to start the experiment. Sample containers and a data logging excel sheet were also prepared in advance of starting each experiment. During the experiments, permeate samples are taken at specified time points to evaluate the protein concentration. When the experiment is complete, the depth filter is either disposed of or kept for further analysis.

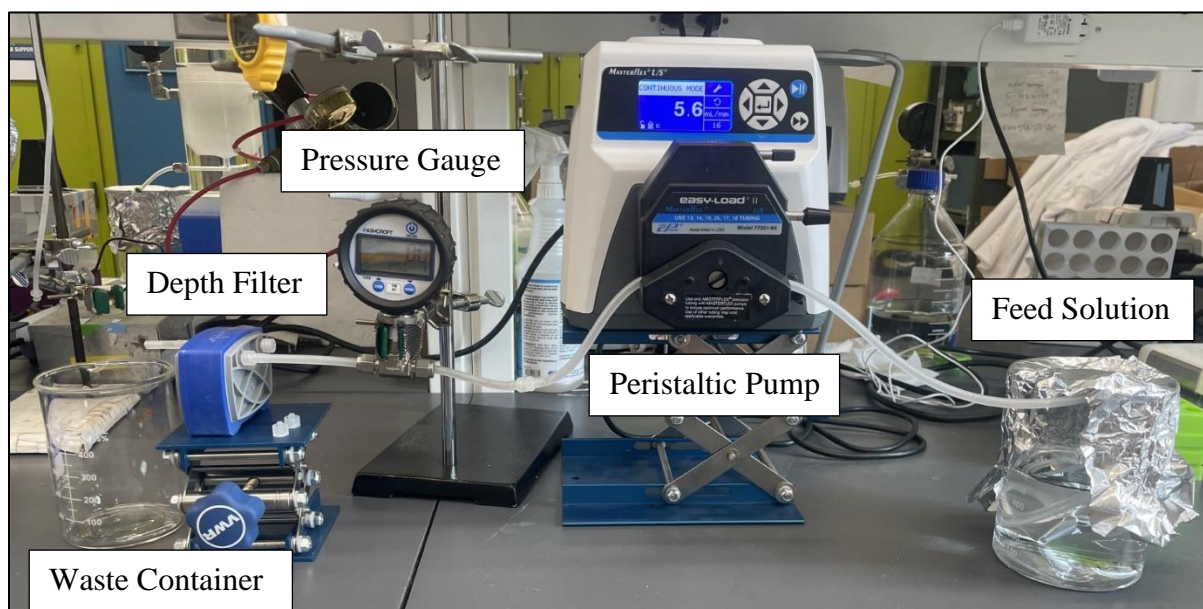


Figure 4. Depth filtration setup.

Table 2. Depth filter summary.

Depth Filter	Size (cm ²)	Medium Composition
A1HC	23	Diatomaceous earth and cellulose
D0SP	23	Synthetic silica particles and polyacrylic fiber
X0SP	23	Synthetic silica particles and polyacrylic fiber

Protein Concentration Measurements

Absorbance measurements were used to determine the concentration of protein in the permeate samples obtained from the depth filter. For each experiment that utilized absorbance measurements, samples of the depth filter permeate were taken at different time points. 0.25 mL

of each of these samples were then aliquoted into a clear bottom 96-well plate. The 96-well plate was then placed into an ultraviolet spectrophotometer (UV-Vis). This device measures the absorbance of light at different wavelengths as it passes through the sample. These measurements were used to produce an absorbance curve and accurately determine the protein concentration. The amount of light absorbed is proportional to the concentration of protein in the sample. This relationship is given by the Beer Lambert Law:

$$A = \epsilon lC \quad (2)$$

where A is absorbance, ϵ is molar absorptivity, l is optical light path, and C is concentration. In this thesis, unless specified otherwise, absorbance was measured at 280 nm, which reflects the presence of protein since their aromatic amino acids (i.e. tryptophan and tyrosine) absorb light at this wavelength.¹⁰

Bradford Assay

Although the UV absorbance is widely used for determining protein concentrations, the CHO HCP solutions contains a wide range of smaller species that also absorb light at 280 nm. In this case, the permeate samples were analyzed using the Bradford Assay. The Bradford Assay is a simple and accurate procedure for determining the concentration of protein in a complex solution. This assay involves the binding of Coomassie Brilliant Blue G-250 dye to proteins.¹ The dye exists in three forms: cationic (red), neutral (green), and anionic (blue). In this work, when the dye is mixed with a solution, it binds to the proteins present and it is converted to a stable unprotonated blue form that is detected by a spectrophotometer at 595 nm.

This assay was performed in a 0.35 mL microplate with protein that ranges from 0.125-1 g/L in concentration. First the dye reagent was warmed to room temperature and mixed. Then, 5 μ L of sample and 250 μ L of dye reagent were added to each well and mixed by repeatedly depressing the plunger of the pipet and then releasing. Each sample was assayed in duplicate and a blank reference sample was prepared containing only the dye and equilibration buffer. The microplate was incubated at room temperature for 5 minutes to 1 hour. The samples were then inserted into the spectrophotometer and their absorbance readings were measured at 595 nm. The absorbance measurement of each sample was averaged and then normalized by subtracting the absorbance of the blank. This process was initially completed with standards of known concentration to develop a calibration curve that provides a linear relationship between absorbance at 595 nm and protein concentration (Figure 3). The ideal standard used in this assay is a purified preparation of the protein being assayed.

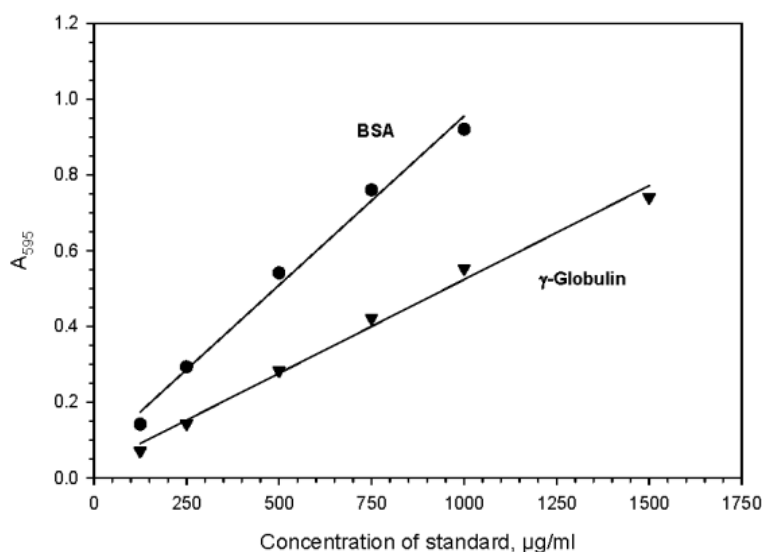


Figure 5. Bradford assay standard curve. Taken from [1].

Chapter 3

Results and Discussion

Effect of pH

In this study, the effect that pH has on the binding capacity of different depth filters was investigated with proteins that vary in pI. The pI of a protein indicates the pH at which it carries no net charge. Therefore, due to the charged surfaces of some depth filters, it is predicted that different pH conditions could impact the ability of the depth filter to bind different proteins so they can be removed from the feed solution. The objective of this study is to quantify the effects of pH and protein properties for different depth filters.

The depth filters used in this study were the A1HC, D0SP, and X0SP. Based on previous experimental studies performed in the Zydney lab, the D0SP and X0SP depth filters rely primarily on electrostatic interactions to remove impurities while the A1HC depth filter relies primarily on hydrophobic interactions. The proteins studied were albumin with an acidic pI (~4.8-4.9), myoglobin with a neutral pI (7), and alpha-chymotrypsin with an alkaline pI (8.8). These proteins were prepared in 20 mM sodium acetate buffer at a concentration of 0.1 g/L and processed through each of the depth filters at a conductivity of 5.0 ± 0.1 mS/cm (the same as the ionic strength of 0.3x PBS buffer). Data were obtained at pH of 4, 4.5, 5, and 6 with the pH adjusted using 5 M NaOH or HCl as needed. The absorbance curve for each run was analyzed to determine the volumetric throughput at which “breakthrough” occurs for each operating condition, where breakthrough is denoted by an increase in the absorbance values in the permeate samples.

Experimental data for albumin processed on the A1HC, D0SP, and X0SP filters are shown in Figure 6. The A1HC and D0SP were operated at pH 4.5 and 6.0 and the X0SP was operated at pH 4 and 5; it was not possible to examine the full range of pH for each of the depth filters due to the limited supply of depth filter capsules. Based on its pI, albumin is negatively charged at pH 6, close to neutral at pH 4.5 and 5, and positively-charged at pH 4. The ratio of permeate sample absorbance to feed absorbance is plotted as a function of the volumetric throughput, defined as the ratio of the total permeate volume (V) to the filter external area (A_f). Albumin breakthrough for the A1HC depth filter occurs at a lower volumetric throughput at pH 4.5 than at pH 6, with the absorbance beginning to increase at $V/A_f = 50 \text{ L/m}^2$ at the lower pH compared to 75 L/m^2 at pH 6. In addition, the binding capacity, defined as the volumetric throughput at which the absorbance equals 50% of its maximum value ($A/A_{\text{Feed}} = 0.5$), increases from 63 L/m^2 at pH 4.5 to 110 L/m^2 at pH 6. The breakthrough curves for the D0SP filter were nearly identical at the two pH values, with binding capacity of approximately 110 L/m^2 at both pH 4.5 and 6. Finally, for the X0SP, breakthrough occurs at a significantly lower volumetric throughput at pH 4 compared to pH 5, with the binding capacity increasing from 200 L/m^2 to more than 350 L/m^2 , respectively.

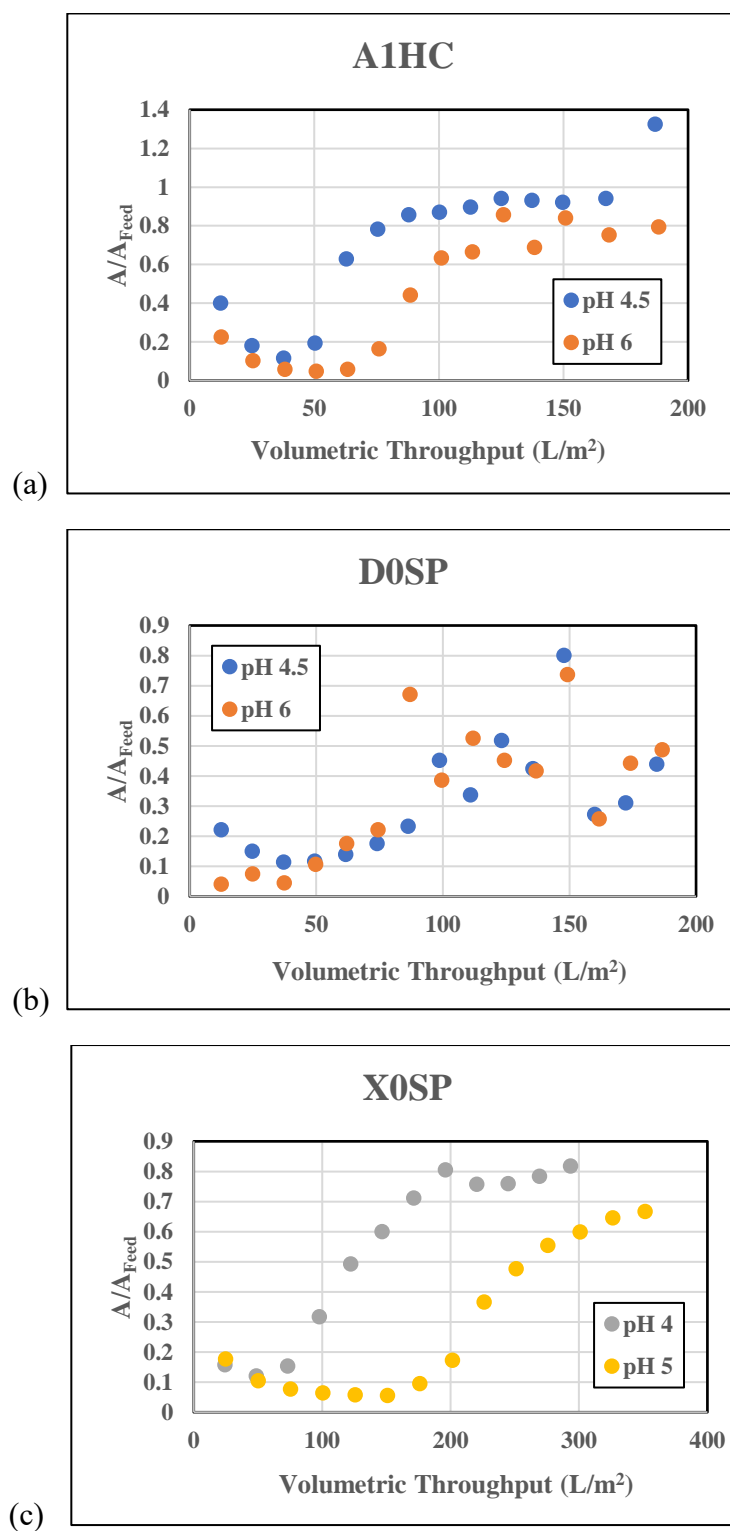


Figure 6. Absorbance profiles for albumin processed at various pH conditions using the (a) A1HC, (b) D0SP, and (c) X0SP filter.

Corresponding results for myoglobin are shown in Figure 7. In contrast to the data obtained with the negatively charged albumin, initial myoglobin breakthrough on the A1HC depth filter occurs at a much higher volumetric throughput at pH 4.5, with the binding capacity decreasing from 67 L/m² at pH 4.5 to only 30 L/m² at pH 6. The breakthrough curves for the DOSP and XOSP filters are essentially independent of solution pH, with binding capacities of about 850 L/m² with the DOSP and 750 L/m² for the XOSP. The slightly smaller binding capacity of the XOSP filter compared to the DOSP filter is surprising since the XOSP and DOSP are made from the same materials, with the primary difference being the effective retention (size) rating of the filters. The smaller pores in the XOSP filter give a much greater total internal surface area, but this did not correspond to a greater binding capacity. This result will require further investigation to determine what is leading to the very similar capacities for these filters.

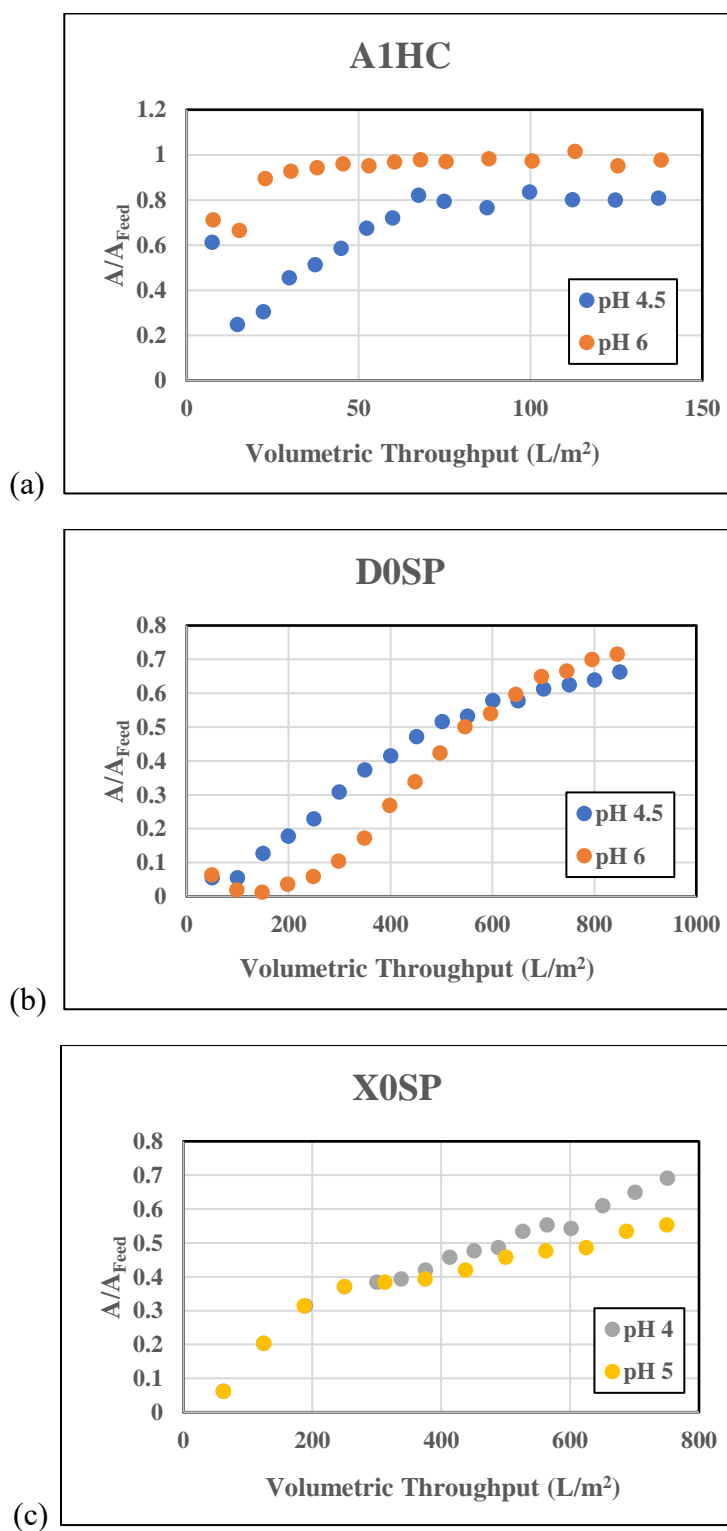


Figure 7. Absorbance profiles for myoglobin processed at various pH conditions using the (a) A1HC, (b) D0SP, and (c) X0SP filter.

Finally, the breakthrough curves for alpha-chymotrypsin processed using the A1HC depth filter at pH 4.5 and 6 are shown in Figure 8. Breakthrough occurs at a slightly lower volumetric throughput at pH 4.5 than at pH 6, with binding capacities of 25 L/m² and 38 L/m², respectively. Alpha-chymotrypsin binding was not examined on the D0SP or X0SP.

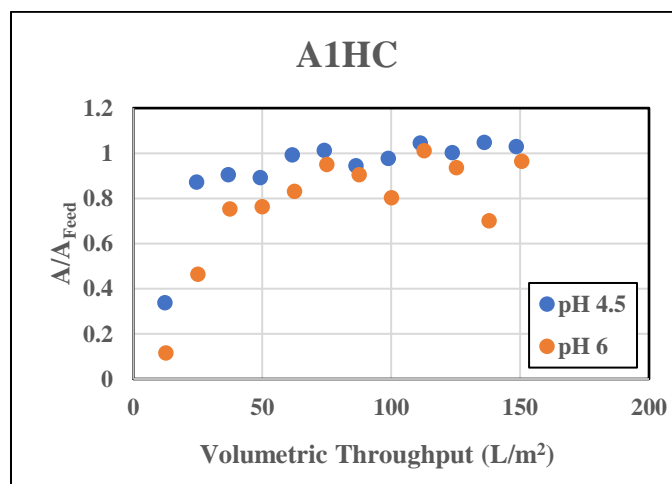


Figure 8. Absorbance profiles for alpha-chymotrypsin processed at pH 4.5 and 6 using the A1HC filter.

Figure 9 summarizes the effects of pH on the binding capacities of the different proteins on the 3 filters examined in this study. As discussed previously, the X0SP and D0SP depth filters are thought to bind proteins primarily via electrostatic interactions. Interestingly, the D0SP showed very similar binding capacities at pH 4.5 and 6 for both albumin and myoglobin, however the binding capacity for albumin was only 110 L/m² compared to 850 L/m² for myoglobin. The different behavior for albumin and myoglobin at acidic pH is consistent with prior expectations. Myoglobin is positively charged at both pH 4.5 and 6 and should thus show strong electrostatic attraction to the negatively charged SP-series depth filters. In contrast, albumin is negatively charged at pH 6 and is close to electrically neutral at pH 4.5, which would

explain the relatively low degree of albumin binding to the D0SP filter under these conditions. The same trend was seen with the D0SP filter, with a binding capacity of 250 L/m² for albumin compared to 750 L/m² for myoglobin. At pH 4 and 5, myoglobin processed on the X0SP resulted in nearly identical absorbance profiles, however albumin binding capacity increased from 120 L/m² to 250 L/m². This supports the physical picture that myoglobin has higher binding capacities than albumin on the D0SP and X0SP as it is positively charged in acidic conditions, enhancing its electrostatic interactions with the negatively charged depth filter media.

In contrast to the strong electrostatic interactions seen with the D0SP and X0SP depth filters, protein binding to the A1HC is based primarily on hydrophobic interactions and should thus be largely independent of the solution pH. For albumin and alpha-chymotrypsin, breakthrough was achieved at a slightly higher volumetric throughput as the pH increased while for myoglobin the breakthrough was achieved at a slightly lower volumetric throughput as pH increased. These small differences in binding capacity could be due to a low level of electrostatic interactions, although it is also possible that changing the pH leads to small conformational changes in the proteins that might affect the magnitude of the hydrophobic interactions with the A1HC.

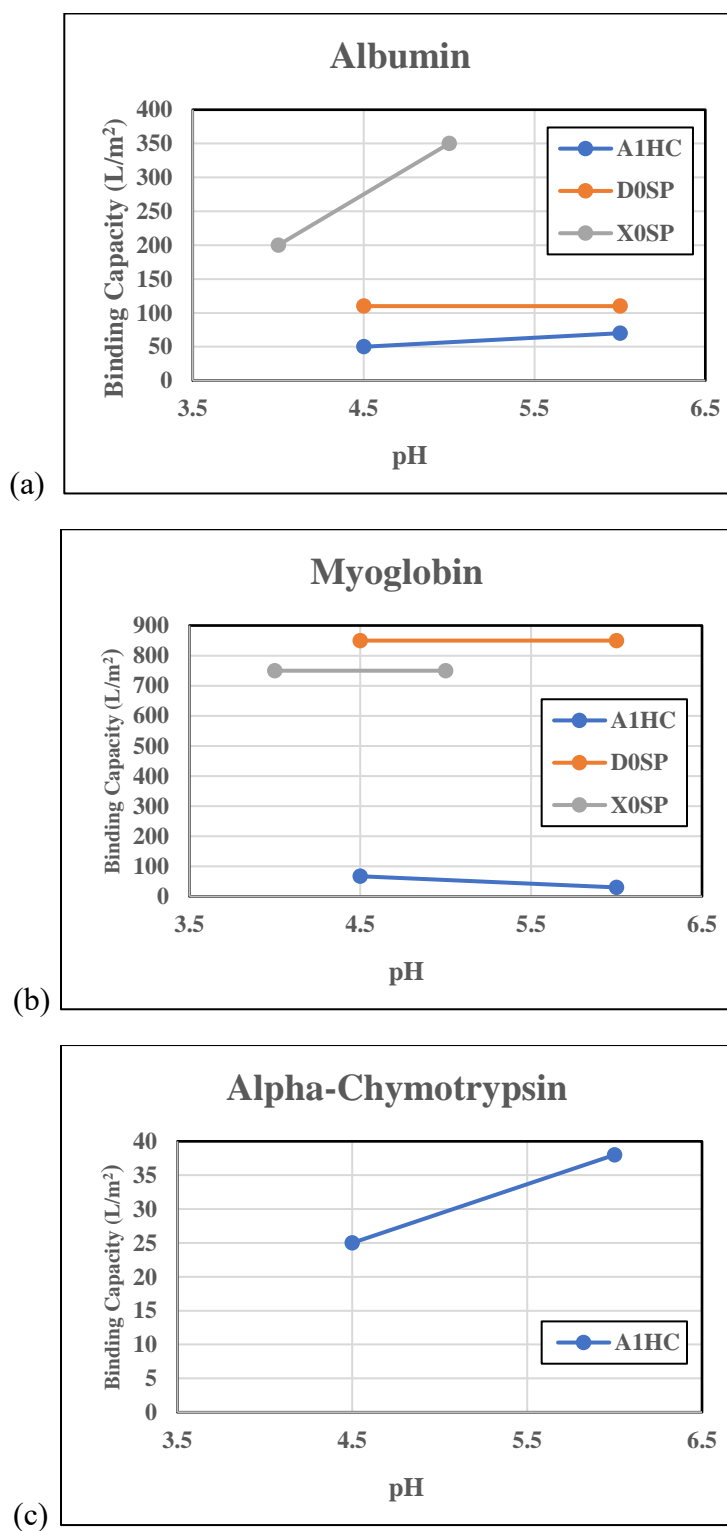


Figure 9. Binding capacities as a function of pH for the different depth filters for (a) albumin, (b) myoglobin, and (c) alpha-chymotrypsin.

Further studies would be needed to draw more quantitative conclusions on the effects of pH on protein binding to the different depth filters. In particular, it would be recommended that alpha-chymotrypsin binding be evaluated on the X0SP and D0SP to see how a protein with an alkaline pI (strongly positively charged) behaves with depth filters that bind primarily via electrostatic interactions. It would also be valuable to study the binding characteristics over a broader range of pH conditions, including alkaline conditions, up until a pH of around 10 where all 3 of the model proteins would have a negative charge.

Effect of Flow Rate

To further examine the binding characteristics of the A1HC depth filter, the impact of operating flow rate on the breakthrough curves was evaluated. The A1HC depth filter was loaded with ovalbumin at a concentration of 0.1 g/L, a pH of 7.4, and a conductivity of 5.0 mS/cm at flow rates of 50, 150, and 300 L/m²/h (usually denoted as LMH). Note that the manufacturer recommends operating the A1HC at a flow rate of 150 LMH, so the conditions examined in this study effectively bracket the normal operating condition for this filter. Figure 10 shows the results, with the absorbance ratio again plotted as a function of the volumetric throughput. It was initially expected that breakthrough would occur at a lower volumetric throughput when using the higher feed flow rate due to the shorter contact time between the proteins and the media. However, this was not observed experimentally as the ovalbumin breakthrough curves were similar at all three flow rates. This suggests that mass transfer is sufficiently rapid within the depth filter media such that even the 300 LMH flow rate provides sufficient residence time for protein binding within the A1HC depth filter. This also indicates that future experiments could be

conducted at 300 LMH without compromising performance, which would significantly reduce the time for the breakthrough studies.

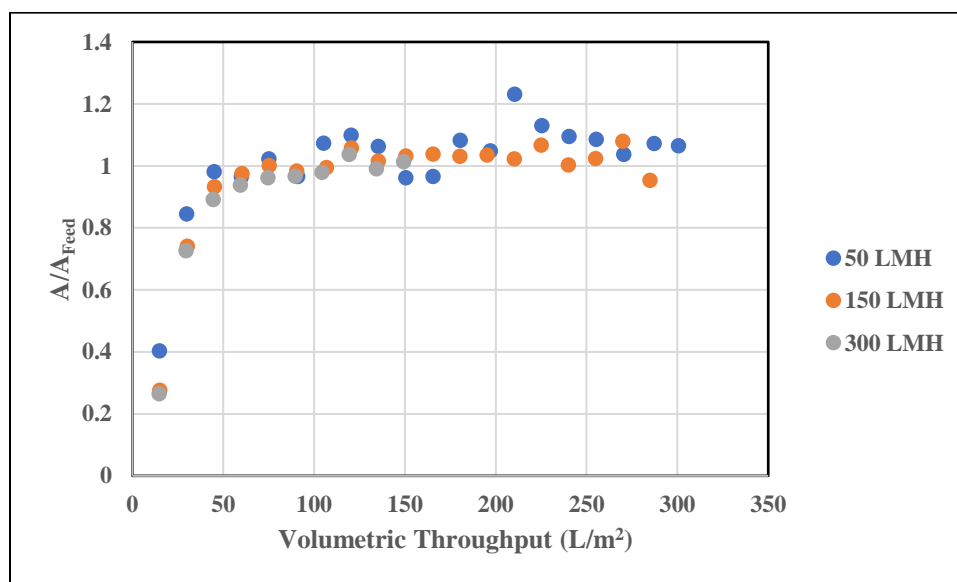


Figure 10. A1HC breakthrough profiles for ovalbumin at 50, 150, and 300 LMH.

HCP Binding

In addition to evaluating the binding capacity of these depth filters with different model proteins, limited experiments were also performed with a mixture of HCP obtained from the cell culture fluid generated from growing CHO cells. The results from these experiments are of direct interest to the biopharmaceutical industry as CHO cells are often used to produce monoclonal antibodies, with current sales of more than \$150 billion/yr.¹¹

This study aimed to determine how the HCP binding capacity for the A1HC depth filter compared to that evaluated using the series of model proteins. Data were obtained using a feed containing HCP at a concentration of 0.12 g/L and a pH of 7.4. This feed was produced by growing CHO-S cells in Freestyle CHO expression media spiked with L-glutamine at 37°C with

cell division occurring every 20-22 hours. The depth filtration was performed identically to previous depth filtrations except the Bradford assay was used to quantify the HCP concentration. Results are shown in Figure 11. The data are highly scattered, but the initial breakthrough occurred at a volumetric throughput of about 20 L/m² with a binding capacity of about 110 L/m². This value is in agreement with the binding capacity evaluated previously in the Zydney laboratory using albumin with this depth filter at similar operating conditions (110 L/m²). This is consistent with the large number of CHO HCP that have pIs between 4.5 and 5.5, similar to the acidic pI of albumin.⁴ This provides further support for using the model proteins to understand the binding characteristics of CHO HCP. Future studies would be needed to evaluate the removal of other product- or process- related impurities and to examine the behavior of different depth filter media with different binding mechanisms.

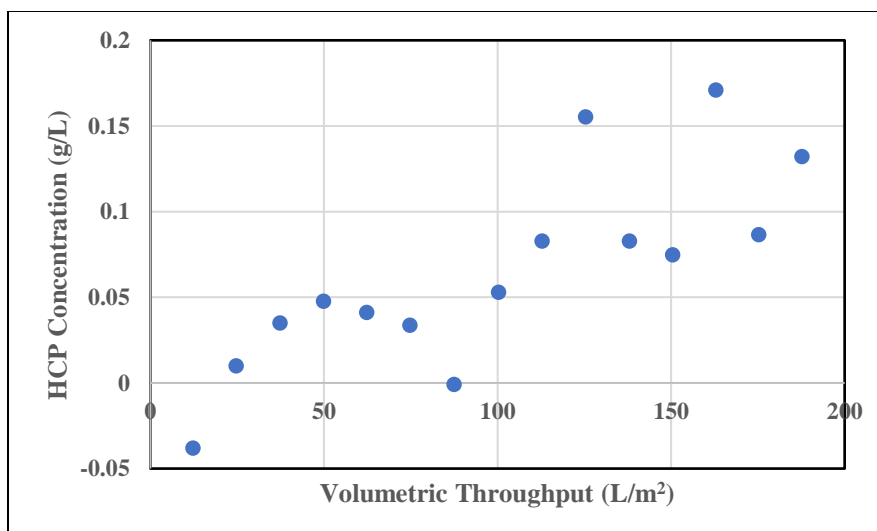


Figure 11. Breakthrough curve for HCP during filtration through the A1HC depth filter.

Chapter 4

Conclusions

Depth filtration is used extensively in the biopharmaceutical industry for the clarification of cell culture fluid and for the removal of protein impurities by adsorptive interactions with the depth filter media. The experimental studies performed in this thesis were designed to provide additional information on how a few commercially available depth filters perform over a range of pH conditions and flow rates using a series of model proteins with different pIs. Data were also obtained with HCP in a clarified cell culture fluid obtained from a CHO cell harvest.

The binding results for the model proteins to the X0SP and D0SP depth filters showed that these two filters bind proteins primarily through electrostatic interactions. In particular, the greatest binding was seen with the positively-charged alpha-chymotrypsin and myoglobin while the lowest binding capacity was obtained with the negatively-charged albumin. However, the binding capacities for the different proteins to the X0SP and D0SP filters were relatively unaffected by solution pH, although this may reflect the relatively small pH range examined in this work.

The binding data with the A1HC depth filter, which tends to bind proteins primarily by hydrophobic interactions, showed binding capacities that were only weakly dependent on either the pH or the protein pI. The binding was also independent of feed flow rate from 50 to 300 LMH. Finally, it was determined that the A1HC depth filter showed similar binding capacity for CHO-derived HCP as that evaluated using albumin.

The data obtained in this thesis is valuable in further understanding the performance characteristics of an important unit operation in the biopharmaceutical industry. The results

provide insights into how the different depth filters are going to perform at low pH conditions based on the protein's pI. The experiments performed with the A1HC demonstrated that this filter can be operated at a feed flow rate at least twice the recommended value without any negative impact on the binding capacity, and the results provide further support for the use of negatively-charged model proteins (like albumin) to probe the binding characteristics of CHO-derived HCP. Future work that could be conducted for each aspect of this study was described in the respective Results and Discussion sections in Chapter 3.

Chapter 5

References

- 1) Bio Rad Laboratories. (n.d.). Quick Start Bradford Protein Assay Instruction Manual. Hercules, California, United States.
- 2) Liang-Kai Chu, Borjueni E. E., Xu X., Ghose S., Zydney A. L. (2023). Comparison of host cell protein removal by depth filters with diatomaceous earth and synthetic silica filter aids using model proteins. *Biotechnology and Bioengineering*. 120(7): 1882-1890.
- 3) Liang-Kai Chu, Wickramasinghe S. R., Qian X., Zydney A. L. (2022). Retention and Fouling during Nanoparticle Filtration: Implications for Membrane Purification of Biotherapeutics. *Membranes*. 12(3): 299.
- 4) Martin Kornecki, Mestmacker F., Zobel-Roos S. (2017). Host Cell Proteins in Biologics Manufacturing: The Good, the Bad, and the Ugly. *Antibodies*, 6(3) 13.
- 5) Ohnmar Khanal, Singh N. (2018). Contributions of depth filter components to protein adsorption in bioprocessing. *Biotechnology and Bioengineering*, 115(8): 1938-1948
- 6) Quigley, G. (2020, October 2). *Depth Filtration*. Retrieved from ErtelAlsop: <https://ertelalsop.com/depth-filtration-2/>
- 7) Salman, S. (2017, December 17). Filtration. Gujrat, Pakistan.
- 8) Scott, K. (1995). *Handbook of Industrial Membranes*. United Kingdom: Elsevier Science.

- 9) Youness Cherradi, S. L.-J. (2018, April 19). Filter Based Clarification of Viral Vaccines and Vectors. *Bioprocess International*. Retrieved from <https://bioprocessintl.com/downstream-processing/filtration/filter-based-clarification-of-viral-vaccines-and-vectors/>
- 10) Anthis N. J., Clore G. M. (2013). Sequence-specific determination of protein and peptide concentrations by absorbance at 205 nm. *Protein Science*, 22 (6).
- 11) Nejatishahidein, N., Zydney, A.L. (2021). Depth filtration in bioprocessing — new opportunities for an old technology. *Current Opinion in Chemical Engineering*, 34: 100746.

ACADEMIC VITA

Kevin Dyke

Education

The Pennsylvania State University, Schreyer Honors College

Bachelor of Science in Chemical Engineering | University Park, PA

Professional Experience

Downstream Process Development Intern (May 2023 – August 2023)

- Regenxbio | Rockville, MD
- Investigated the influence of resin ionic capacity on the performance of anion exchange chromatography and the source of observed yield loss during Regenxbio's platform downstream purification process.

Downstream Research & Development Scientist (January 2022 – July 2022)

- Janssen Pharmaceuticals | Malvern, PA
- Evaluated how to apply new technologies and methods to improve the process of protein purification, while assisting in the development of a supplemental vaccine for respiratory syncytial virus variant B (RSV-B).

Undergraduate Research Assistant (May 2021 – December 2023)

- The Pennsylvania State University | University Park, PA
- Studied the use of depth filters for the removal of host cell proteins in the purification of monoclonal antibodies and the effect pH has on binding capacity (Dr. Andrew Zydney).
- Studied the antimicrobial capabilities of the *Moringa oleifera* protein and its application in developing countries as a low energy and cost method of water purification (Dr. Stephanie Velegol).

Awards & Scholarships

- Dean's List every semester.
- Leighton and Lorene Riess Scholarship in Chemical Engineering.

Leadership & Organizations

- *Omega Chi Epsilon Academic Outreach Chair*: Chemical engineering honor society focused on recognition, investigation, service, comradeship, and professionalism. Provided a connection between students and professors and helped organize professional development events.
- *Chem E Car Club Member*: Collaboratively worked as a team to design a car that travels a desired distance using only chemical reactions.
- *Tau Beta Pi Member*: Engineering honors society based on distinguished scholarship (top 8th of engineering students in class) and exemplary character.
- *American Institute of Chemical Engineers (AIChE) Member*
- *Penn State Men's Lacrosse Club*: Two-year member of the tea

Skills

- Expertise in standard laboratory techniques (chromatography, filtration, flocculation, distillation, crystallization, NMR, IR) and instruments (AKTA, pipet, stir/hot plate, balance, etc.).
- Experimental design, data analysis, communication, teamwork, and presentation.
- Proficient in Microsoft, Solid Works, Mathematica, MATLAB, Empower, Biovia, Unicorn v7.6, and JMP.